In: Polarons: Recent Progress and Perspectives
Editor: Amel Laref
ISBN: 978-1-53613-935-8
© 2018 Nova Science Publishers, Inc.

Chapter 5

ANHARMONICITY, SOLITON-ASSISTED TRANSPORT AND ELECTRON SURFING AS A GENERALIZATION OF POLARON TRANSPORT WITH PRACTICAL CONSEQUENCES

Manuel G. Velarde[1,*] and E. Guy Wilson[2]
[1]Instituto Pluridisciplinar, UCM, Madrid, Spain
[2]School of Physics and Astronomy, Queen Mary University of London, London, UK

ABSTRACT

We discuss a generalization of the polaron concept to include soliton assisted transport. Electron surfing with a lattice soliton is described. The generalization also offers a clear case of mechanical control of electrons at the nanolevel. Building upon such a generalization, the concept of a solectron was introduced and a new solectron field effect transistor (SFET) has been designed, which relies on the ballistic flight of the solectron at a velocity independent of the field, and even in a zero field. This opens up the possibility of low energy computation.

Keywords: anharmonicity, solitons, solectrons, electron surfing, hyperconduction, SFET

1. INTRODUCTION

The polaron concept originated in Landau's idea [1] of self-trapping for an electron in the polar lattice distortion it creates when added as an excess charge to an (originally) ionic crystal, due to the Coulomb interaction. He considered that such a compound (electron and induced polarization field) was the actual carrier in charge of transport, hence of electricity in the presence of an external electric field. The concept also applies to the self-trapping of a (positive) hole. Later on, the concept was refined and redefined, first by Pekar [2, 3], Landau

* Corresponding Author address. Email: mgvelarde@pluri.ucm.es.

Complimentary Contributor Copy

and Pekar [4] and, subsequently, by Pekar [5] and collaborators [6, 7]. Eventually it was made complete by Fröhlich [8, 9], Holstein [10], Feynmann [11] and others [7, 12-17] thus leading to the quantum transport theory in solid state physics [18-24].

The building bricks of the polaron as we consider it today are, on the one hand, the crystal Hamiltonian with harmonic interactions (hence the linear mechanical elasticity) underlying the phonons as quantum (stationary) wave excitations in the lattice extending from one end to the other of the crystal. The other item is the nonlinear electron-phonon interaction. Thus a polaron, also denoted as a quasi-particle, is a dressed electron or an electron surrounded by a cloud of (a few) phonons. Indeed from a field theoretic viewpoint, the induced polarization appears as a cloud of virtual phonons around the electron. Needless to say, the polaron is a genuine electronic excitation, as the electron causes the polaron to exist.

From 1960 to 1980, several lines of polaron extension occurred. On the one hand, there was the discovery of (dopable) conducting polymers that eventually led to the Nobel Prize in 2000 to Heeger, MacDiarmid and Shirakawa and, more relevant to us, the introduction of the so-called SSH Hamiltonian by Schrieffer and colleagues [25, 26] to account for such conduction of otherwise originally (when undoped) insulator-like synthetic materials, which were later on denoted as "synthetic metals". The second line was the introduction of the electro-soliton concept by Davydov to account for transport and related phenomena in biomolecules [27-29]. The third line was the numerical "discovery" and spectacular development of the soliton concept, coinage by Zabusky and Kruskal [30], with work – analytical and numerical – by many others, among which included Toda [31, 32]. The latter offered a Hamiltonian model with anharmonic interactions between the units that he had completely been solved analytically. Solitons are mechanical excitations in a crystal lattice that tend to be of significance past the Dulong-Petit plateau in the specific heat against temperature, thus indicating their more classical than quantum character [33].

The SSH line of thought [25, 26] builds upon the harmonic interactions between units, the degeneracy of the ground state of polymers like trans-polyacetylene (tPA) described by a quartic contribution added to the originally harmonic Hamiltonian, and the tight binding approximation to account for band flow as means of electron transport. tPA (like many other polymers in the same class) was a poorly crystalline material that upon doping changed from an insulator-like behavior to copper-like metallic conductor. When electrically conducting, it was first suggested that electron transport was based on the existence of solitons/kinks, otherwise denoted as topological solitons, due, indeed, to the degeneracy of the ground state. Later on, the transport was rather associated to polaron or bipolaron transport. Still today no one mechanism seems to apply to tPA over the whole range of doping.

Davydov [27-29] was able to identify bio-related lattices with characteristics capable of leading to soliton-bearing Hamiltonians – at variance with the SSH theory for tPA not based upon degeneracy of the ground state- whose solution he offered. Unfortunately his predictions – at that level – were not supported by experiment nor did they survive going to temperatures beyond a few K, though this result was not without criticism [34-38]. Then in the 1980s and 1990s, Davydov [29, Ch. 6, 37] and colleagues [39-41] extended the original theory by using Hamiltonians with cubic and quartic anharmonic interactions thus allowing for supersonic soliton-assisted charge transport with, once more, all results studied at zero K.

In an independent approach, already during the 1970s, Zmuidzinas [42, 43] also explored the idea of going beyond polaron-assisted transport. In particular, building upon the Fröhlich

Complimentary Contributor Copy

approach (distortion dependent on-site energy) he analyzed a Hamiltonian with quartic interactions and also advanced the concept of soliton trapping electrons thus leading to electron surfing transport. Zmuidzinas estimated the activation energy of a lattice soliton in the range of 1eV (quite a high temperature 1.16×10^4K; earlier we mentioned that solitons, e.g., in a Toda lattice, tend to appear past the Dulong-Petit plateau in the specific heat [33]) though he suggested the possible observation of this form of soliton-assisted hyperconduction in the range of tens of degrees K.

During the 1990s, following the path set by Davydov, Kadantsev and colleagues [44, 45] considered a Hamiltonian with quintic interactions in a lattice in interaction with a thermal bath (non-zero T). The quintic interaction and the heating permitted to sustain solitons capable of trapping electrons and hence soliton-assisted transport at non zero K.

In the 1980s and 1990s, Wilson and Donovan and colleagues [46-49] explored the experimental characteristics of a non dopable, perfectly crystalline polymer, poly-diacetylene (PDA) and sulphonate derivatives (PDATS). Donovan and Wilson [46] found, by experiment in PDA, a photocarrier to travel at a velocity close to the sound velocity, when pulled by an electric field. However, the velocity was independent of field, even over four decades of field research. Moreover, at the lowest field, the velocity was greater than what would be found in any semiconductor at the same field. (In conventional semiconductor language, the low field mobility was ultra-high, greater than 20 $m^2\ s^{-1}\ V^{-1}$). The carrier had thus a low dissipation of energy to the lattice. The carrier was ballistic. The backbone of PDA crystal is made of π conjugated carbon chains. The chains are long, straight and parallel for macroscopic distances. The lowest electronic excitations belong to the backbone chains. The chains are separated by a (electronically) large distance (0.7 nm). Thus they form ideal one dimensional semiconductor. Optical absorption above the band gap (2.4 eV) created electron and hole photocarriers. The theory developed by Wilson [50] built upon the SSH approach –with, however, no degeneracy of the ground state in PDA- and later found having similarity to Davydov's approach (distortion dependent electron transfer). He advanced the concept of solitary wave acoustic polaron (SWAP) as charge carrier clearly extending the original polaron realm into the soliton-like assisted transport, and quite a different mechanism for transport relative to the dopable tPA family. Yet in all cases so far mentioned, though the lattice dynamics enters well beyond the simplest induced lattice polarization distortion, we still have genuine electronic excitations, as without the added excess electron there is no evidence of the crystal excitation.

Starting in 2005, in an independent approach, Velarde and colleagues [51-56] considered from the very beginning a Hamiltonian with Morse anharmonic interactions and developed a theory that, besides providing genuinely new predictions, embraced many of the results obtained by earlier mentioned authors, emphasizing the significance of supersonic solitonic motions. In Emin's book [17] there is discussion of the role of anharmonicity in polaronic problems but we suggest it does not apply here, for it belongs to a different line of thought than the one presented here. The dynamic bound state of an added excess electron to a [Morse (Toda)] lattice soliton was denoted solectron [51, 55], as the natural extension of the Landau-Pekar polaron concept where the (nonlinear) mechanical lattice excitation dominates and permits control of an added excess electron even in the absence of an external electric field [56]. In [57], in a certain sense interpolating between the theories of Zmuidzinas [42, 43] and Wilson [50] (albeit retaining the discrete character of the lattice throughout; both Zmuidzinas and Wilson resort to continuum approximations), there is a discussion of the role of the

Complimentary Contributor Copy

increasing strength of electron-lattice (phonon) interaction leading from polaron to solectron. Their results also included predictions about the stability of solitons and solectrons up to physiological temperatures, e.g., bio-related lattices (ca. 300K) [58-60]. They also considered cubic and quartic interactions, and the onset of pairing of two solectrons (bisolectron concept as extension of the bisoliton concept of Davydov and Brizhik [61-65]).

The outline of the chapter is as follows. In Section 2 we discuss the implementation of the solectron concept, in the form of solitary wave acoustic polaron, as done by Wilson [50]. Consequences of such implementation are sketched and some limitations of the theory indicated. Then Section 3 deals with the implementation of the solectron concept based upon the anharmonicity of the lattice interactions thus extending Wilson's study. The concept of electron surfing on discrete lattice solitons is recalled and some of its significant consequences are discussed. In Section 4 a novel filed effect transistor based upon the solectron concept (SFET) is succinctly described.

2. SOLITON WAVE ACOUSTIC POLARON THEORY

We discuss now a solectron-like theory produced by Wilson [50] (then called a solitary wave acoustic polaron, or (SWAP) in an attempt to explain extraordinary experimental results found by Donovan and Wilson [46-49] on charge motion in a highly electronically one dimensional system PDATS.

PDATS is a perfect crystal comprised of parallel conjugated polymer chains. The chain backbones, which host any extra electron added, are a large distance apart from each other; thus, such extra electron resides in a perfect electronically one dimensional world. They found an extra electron, photo injected, to travel at a constant velocity, no matter what the value of the applied field. This was so for a variation of field by four orders of magnitude. Moreover the distance of travel in such fashion could approach a millimeter.

The theory was later learned to be similar to soliton-like theories of Davydov. But the theory attempted to use experimental values of all parameters to give results which had values to compare to experiment, and to predict experimental behavior. Attention was also paid to the stability of the solectron, and to the dissipation to an external phonon bath.

The main conclusion was that, at room temperature, a solectron of thermal energy kT, travelled as a ballistic particle, with a velocity just below the sound velocity. An applied field made little change to this velocity. Dissipation by acoustic phonon emission is forbidden. Rather, ambient acoustic phonons can bounce off the solectron and extract energy. But the probability of this process was shown to be very weak. Thus, the theory seemed to give a good account of the experimental results.

Both the experimental results, and the theory, are utterly different than the situation in three dimensional materials such as silicon.

The theory begins with the Su, Schrieffer, Heeger (SSH) Hamiltonian [25, 26], but used here to describe one extra electron on a polymer chain,

$$H=\left(\frac{1}{2M_a}\right)\sum_n\left\{p_{a,n}^2+\left(\frac{M_aS^2}{a^2}\right)\left(u_{a,n+1}-u_{a,n}\right)^2\right\}-\sum_n t_{n+1,n}\left(c_{n+1}^*c_n+c_n^*c_{n+1}\right) \tag{1}$$

Complimentary Contributor Copy

where

$$t_{n+1,n} = t_0 - \alpha\left(u_{a,n+1} - u_{a,n}\right) \tag{2}$$

The lattice part of H describes the momentum, $p_{a,n}$ and displacement, $u_{a,n}$ of the n'th unit call, of mass M_a. a is the unit cell size, and S is the sound velocity. While the unit cell of PDA has 4 carbon atoms along the backbone, there is considerable greater mass residing in the TS side groups of the polymer. The side group is $-CH_2$ $-O-SO_2$ $-C_6H_4$ $-CH_3$. There are 46 atoms in the unit cell of a single chain, of which only 4 are in the carbon backbone. A long wavelength acoustic wave in the chain direction will give compressions and rarefactions of the whole mass of the cell.

Values of these parameters $M_a$and a are given in Table 1. The value of unit cell length a is from the X ray structure of Kobelt and Paulus [66]. Donovan and Wilson [46] estimated the sound velocity $S \approx 5 \times 10^3$ m/s from values of bulk modulus, $c \approx 5 \times 10^{10}$ N/m^3 [67] and density $\rho = 1.48 \times 10^3$ kg/m^3 [65]. The density is from X ray structure determination, and so accurate. Derivation of S from $S - (c/\rho)^{1/2}$ is very fraught in an anisotropic material, so S is not accurate. Lochner et al. [67] measured the changes of lattice parameters with hydrostatic pressure, observing anisotropy. The elastic modulus C3 = 1.88×10^{10}N/m^2. This gives $S = 3.6 \times 10^3$ m/s in the chain direction, which is probably a better estimate of S, and used in Table (1).

Now consider the electron part of H. When undeformed, the electron resides in a Bloch band, the lowest unoccupied band of the PDA. A band structure calculation of Wilson [69] gave equal electron and hole band masses of (1/4) the free electron mass. Consider a chain of N unit cells. All the N states of a band, e.g., using the whole Brillouin zone, can be used to form N Wannier states. Such states are localized around the 4 carbon atoms of the backbone of the unit cell. They are identical within each cell, and form a Complete Normal Orthogonal Set. These states are used as the basis states of the electronic part of the Hamiltonian. That is

$$\phi_n = c_n^* \mid O >$$ (3)

is a Wannier state ϕ_n at cell n produced by the creation operator c_n^*. These basis states are molecular like, but come from the whole band. They are not some fictitious sub molecule formed by arbitrarily chopping up the chain.

Consider now the term, $t_{n+1,n}$, in the Hamiltonian, which transfers the electron between adjacent Wannier states. In the undeformed chain then H creates a band, and the bottom of the band has an effective mass given by

$$m = \frac{\hbar^2}{2a^2 t_0} \tag{4}$$

Complimentary Contributor Copy

Table 1. Numerical values for Polydiacetylene (PDA)

Quantity	Symbol	Value	Reference/Comment
unit cell length	a	0.49 nm	
unit cell mass	M_a	7.0×10^{-25} kg	includes side chain mass
sound velocity	S	3.6 km/s	
electron band mass	m	2.3×10^{-31} kg	1/4 of free electron mass
deformation potential	D_a	3.7 eV	
solectron width parameter	γ_{0a}	9.59×10^{-2}	Eq. (9)
solectron energy parameter	U_a	5.80 meV	Eq. (12)

Thus, the value of $t_0$can be found from the band mass.

The deformation potential $D_a$is a measure of the shift of the band edge with dilation, and is used in semiconductor physics to measure the strength of the electron acoustic phonon interaction, and to model the electron scattering probability, by acoustic phonons and hence to model the mobility. The SSH Hamiltonian measure of the effect of dilation is due to α, where α multiplied by the bond stretch is the change of the transfer integral. Then

$$D_a = 2\alpha a. \tag{5}$$

Thus, the value of α can be found if the deformation potential is experimentally known. Dilation can be carried out by mechanical stretching, and band edge shifts resulting detected optically. However, in PDA, excitons dominate the optical absorption, while the electron hole interband absorption is a weak feature. Dilation of a sample in the chain direction by mechanical stretching gives an observed shift in the exciton energy. This shift is 3.7 eV/m [69]. If the associated electron band edge is shifted the same amount, then $D_a = 3.7$ eV.

This estimate of D_a and hence α is an approximation. For the exciton binding energy may shift also. And the shift may be due to hole band edge shift as well as electron band edge shift. This concludes discussion of the experimental numerical parameters for the Hamiltonian.

The solectron electron state ψ is of the form

$$\psi = \sum_n a_n \phi_n \tag{6}$$

An analytic form for the amplitudes a_n, and then all properties of the solectron, can be found, in the continuum limit, and assuming the adiabatic approximation. For the electron, then the localized electron amplitudes are

$$a_n = (\gamma_a/2)^{1/2} \operatorname{sech}[\gamma_a(n-n_0)] \tag{7}$$

where

$$\gamma_a = \gamma_{0a}/(1-\beta^2) \tag{8}$$

Complimentary Contributor Copy

$$\gamma_{0a} = \left(D_a^2 m a^2\right)/\left(2M_a S^2 \hbar^2\right) \tag{9}$$

and

$$\beta = v/S \tag{10}$$

Here v is the solectron velocity. The energy of the electron in this state is

$$\varepsilon_e = -U_a/\left(1-\beta^2\right)^2 \tag{11}$$

where

$$U_a = \left(m/8\hbar^2\right)\left(D_a^4 a^2/M_a^2 S^4\right) \tag{12}$$

Corresponding to this electron state there is a localized displacement of the unit cell positions given by

$$u_{a,n} = -\left[D_a a/2M_a S^2\left(1-\beta^2\right)\right]\tanh\left[\gamma_a\left(n-n_0\right)\right] \tag{13}$$

The lattice energy due to this distortion is

$$\varepsilon_L = \left(2U_a/3\right)\left(1+\beta^2\right)/\left(1-\beta^2\right)^3 \tag{14}$$

The resultant and total solectron energy is

$$\varepsilon = -\left(U_a/3\right)\left(1-5\beta^2\right)/\left(1-\beta^2\right)^3 \tag{15}$$

Thus, all properties of the solectron are numerically determined by these equation and the experimental parameters of Table (1). The values of the resulting solectron width parameter, γ_{0a}, and energy parameter, U_a, are also given in Table 1.

As the velocity v increases from zero, the total energy increases. The solectron narrows, the electron becomes more tightly bound within the distortion of the lattice, and the lattice distortion energy increases. As v approaches the sound velocity S then the energy rises asymptotically to infinity. If a force F is applied to a solectron at rest, by means of an applied electric field, the energy increases, and the velocity increases towards the sound velocity.

It is desirable to know the precise effect of the field on the solectron dynamics and internal structure. It is interesting that the solectron is described by the Lagrangian L_s where

$$L_s = \left(U_{0a}/3\right)/\left(1-\beta^2\right)^2;\beta = V/S;V = dX_s/dt \tag{16}$$

The solectron momentum P_s conjugate to the solectron position X_s is

Complimentary Contributor Copy

$$P_s = \partial L_s / \partial V = \left(4U_{0a}/3S\right)\beta/\left(1-\beta^2\right)^3 \tag{17}$$

The solectron Hamiltonian H_s is then

$$H_s(P_s, X_s) = VP_s - L_s \tag{18}$$

It is the case that H_s is identical to the solectron total energy, confirming that the Lagrangian is correct.

A force F adds an extra term $-FX$ to the Hamiltonian. The Hamilton equation for dP/dt then gives

$$dP_s / dt = -\partial H_s / \partial X_s = F \tag{19}$$

Thus, an applied force changes the value of solectron momentum P_s in a manner linear in time. Thus, the value of all properties of the solectron in response to an applied field can be determined. There is no explicit expression for the energy against momentum P_s.

Figure 1 shows the energies making up the solectron as a function of its velocity. At room temperature T then the thermal energy kT is 25 meV. Thus, a solectron in thermal equilibrium is already moving at around 70% of the sound velocity. The electron is more tightly bound than in the solectron at rest.

Figure 2 shows the total energy and velocity as a function of the momentum. One can now follow the response to an electric field applying the force F to the solectron. Suppose the solectron is initially at rest, having zero momentum, and then a positive force is applied. The momentum increases at a uniform rate in time. The velocity increases, linearly in time initially, but asymptotically approach the sound velocity. If the field is now reversed, the momentum decreases uniformly in time, and eventually goes negative. The velocity accordingly diminishes, goes through zero and then reverses.

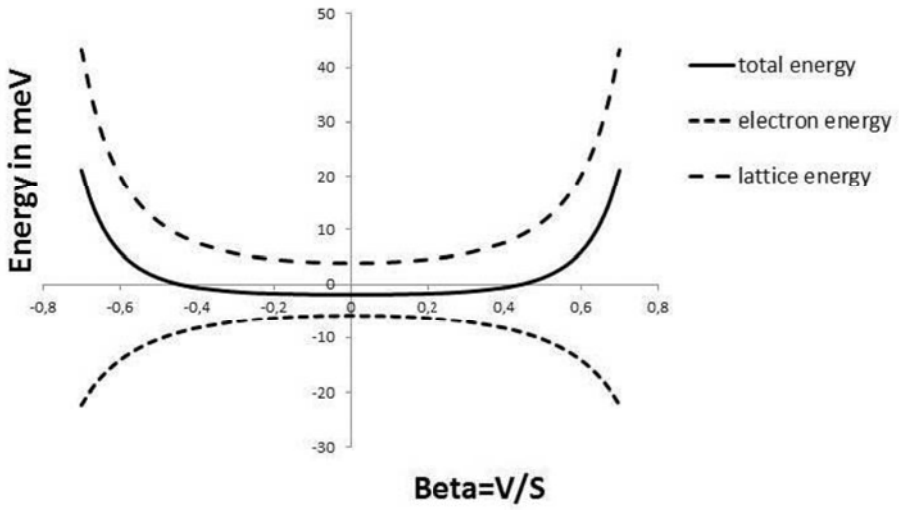


Figure 1. Electron energy, lattice energy and total energy, in meV against $V/S.kT$ is 25 meV.

Complimentary Contributor Copy

In anticipation of Section 4 it is considered an ensemble of solectrons under a conducting source or drain. It is imagined that solectrons of a range of energies around kT will leave these regions. Their subsequent motion in response to fields can be determined from the above considerations. In particular, a field opposing the motion can stop and then return a solectron to the drain.

The plotted values of momentum are helpfully related to the Brillouin zone boundary wave vector K_{BZ} and momentum P_{BZ}, which are given by

$$P_{BZ} = \hbar K_{BZ} = \hbar(\pi/a) = 0.00420(meV)(s/m) \tag{20}$$

In Figure 2 it is seen that a Solectron of thermal energy kT has a momentum of about 0.012 (meV)(s/m) which is about 2.9 P_{BZ}. Thus the solectron K value lies well beyond the first Brillouin zone boundary. This in turn gives a de Broglie wavelength $\lambda = 0.69a$. The wavelength is less than the unit cell size.

Consider now the width of the solectron, which can be taken as $(2/\gamma_a)$ unit cells. For a solectron at rest this gives a width of 20.9 unit cells. For a solectron of thermal energy and velocity 0.69S the width shrinks to 10.7 unit cells. The large size of the solectron compared to the unit cell size is a justification for using the continuum limit approximation in deriving all the results. The size of the solectron is much greater than its de Broglie wavelength. Thus it behaves as a massive ballistic large particle and most unlikely to scatter at Brillouin zone boundaries.

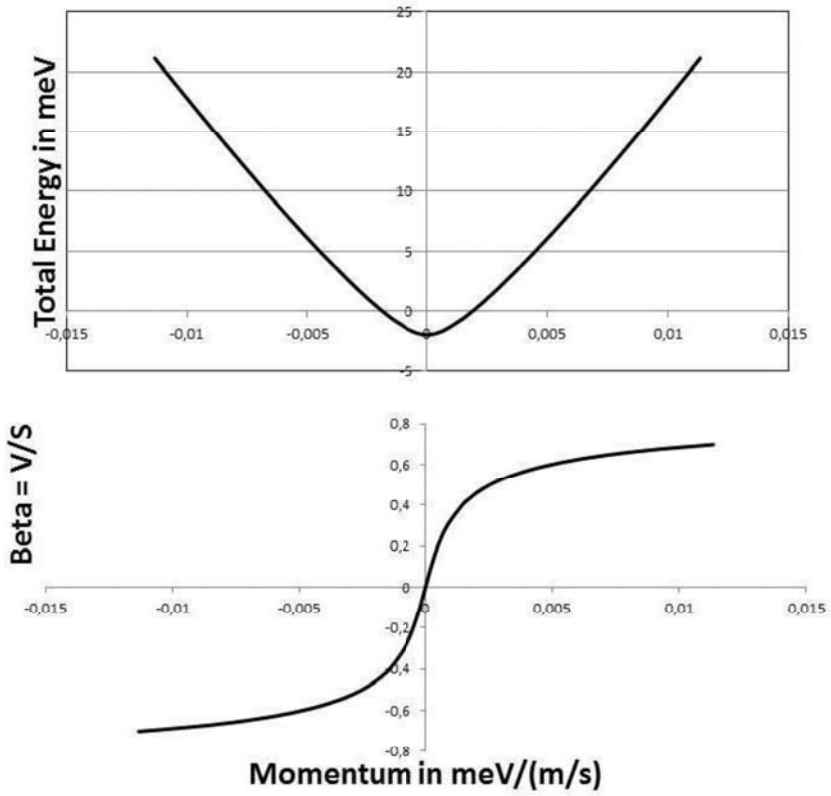


Figure 2. Solectron total energy in meV, and velocity V/S, against solectron momentum, in (meV)(s/m).

Complimentary Contributor Copy

3. NONLINEAR ELASTICITY, LATTICE SOLITONS AND ELECTRON SURFING

3.1. Potential Interactions. Going beyond the Harmonic Potential

In the preceding section, the interaction potential as lattice intersite interaction used to construct the theory is the harmonic one, as expressed in the second term of the left hand side of (1). We have shown how far we can go in the consideration of a generalization of the polaron concept by introducing the concept of soliton acoustic wave polaron (SWAP). The latter came as consequence of the continuum approximation to the originally discrete lattice problem after the electron-lattice interaction was introduced. Now we consider a further albeit different extension –still in 1d- obtained by replacing the harmonic with the Morse potential which is anharmonic. However, at variance with the above described SWAP approach we shall strictly be retaining now the discrete character of the lattice throughout and we shall not consider the addition of the electron and hence no electron-lattice interaction in a first step. The Morse lattice intersite potential is

$$V(r) = (a/2b)(e^{-2br}-2e^{-br}) = D(e^{-2br}-2e^{-br}) \tag{21}$$

where, for later convenience, here r denote interatomic distance, D is the potential depth (or dissociation energy; $D = a/2b$, with a and b here denoting, respectively, the linear Hooke elastic constant (corresponding to the factor MS^2/a^2 in Eq. 1) and the (anharmonic) stiffness of the intersite "springs" (Figure 3). The lowest order hence harmonic vibration is $\omega_M = (ab/M)^{1/2} = (2Db^2/M)^{1/2}$. Referring to relative intersite motions we set $q_n = b(u_n-\sigma)$, with σ here indicating the equilibrium value. To be recalled is that in 1d the kinetic energy is twice the potential energy.

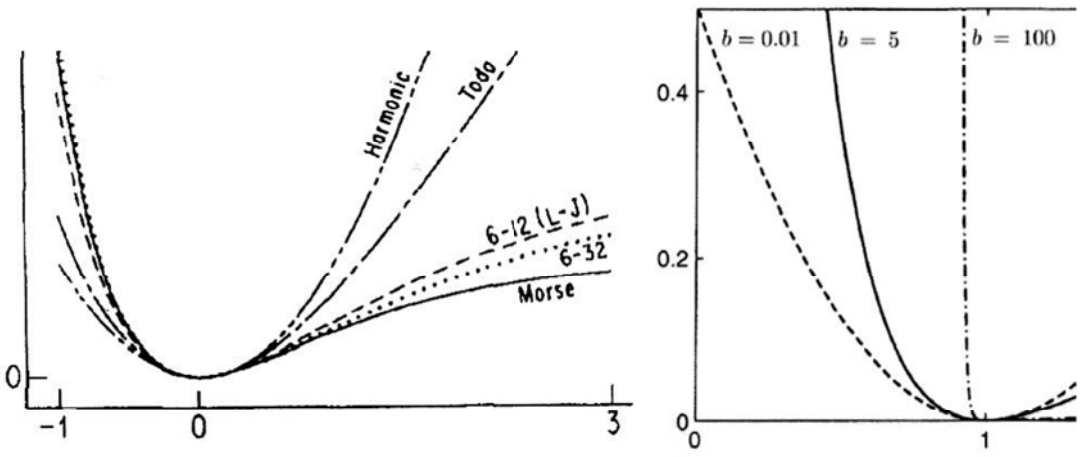


Figure 3. Interatomic potentials. Left panel: Harmonic, Toda [32], (6-12) and (6-32) Lennard-Jones and Morse interactions. Right panel: stiffness of the Morse potential from harmonic (b going to cero; b = 0.01) to "hard sphere" (b going to infinity; b = 100) interactions. Noteworthy is the lack of validity of both the harmonic and Toda interactions when dealing with certain material characteristics besides having an unphysical attractive component as the equilibrium lattice interatomic distance grows.

Complimentary Contributor Copy

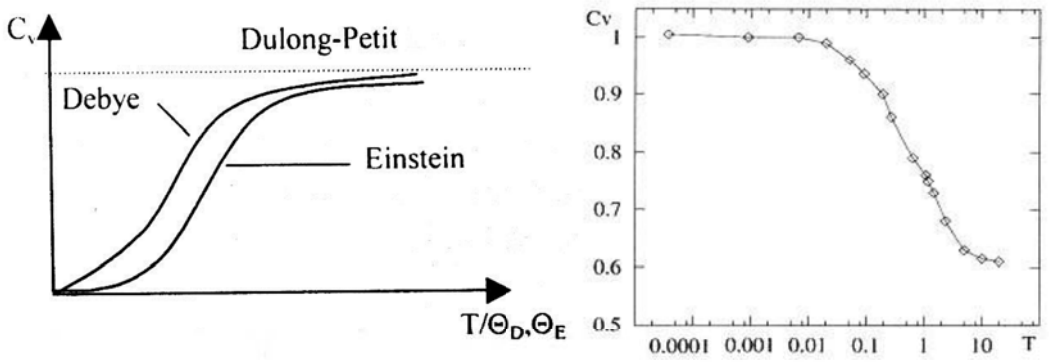


Figure 4. Specific heat C_v, at constant volume/length against absolute temperature T, in dimensionless units (rescaled with the Morse well depth). Left panel: sketch of the predictions of Einstein and Debye theories, at low temperatures, ending in the classical Dulong-Petit plateau at high enough temperatures (curves rescaled with their corresponding Debye and Einstein temperatures). Right panel: computer results for a Morse lattice of the Dulong-Petit plateau and its continuation as the temperature increases on the way to melting. It is along the slopped region (0.1-1) where solitons in such crystal lattice are of significance as also indicated by the dynamical structure factor depicted in Figure 5.

Noteworthy is that if rather than the Morse potential we use the Toda potential (Figure 3, left panel), the dynamical lattice system is integrable, that is, we explicitly know its exact analytical solution [32]. For the non integrable case with Morse interaction the solution has been obtained numerically and the results are within ten percent error relative to the exact Toda solutions [33]. The lattice solitons, for both the Toda and the Morse lattice intersite potentials, are predicted to be of significance in the slopped region of the specific heat (at constant length), against temperature, past the Dulong-Petit plateau (Figure 4, right panel). This result is confirmed by the computation of the dynamic structure factor (space-time correlation of density fluctuations in thecrystal) (Figure 6), a typical quantity for experiments with thermal neutron scattering.

As noted above, the interaction potential (21) refers to change in relative intersite distances and hence longitudinal motions. Noteworthy is that the Morse potential is a "soft" potential in the sense that when widening the intersite/atomic separation it is of weaker strength than the linear Hooke/harmonic spring, and hence the frequency of small amplitude oscillations around the minimum decreases with increasing amplitude. The converse case is considered as a "hard" potential. It turns out that discreteness in a lattice provides bounds and gaps to the spectrum of linear oscillations whereas nonlinearity makes the amplitude of oscillation frequency-dependent. The combination of discreteness and nonlinearity has led to the finding of a form of local excitation denoted discrete breather (DB), otherwise said intrinsic localized mode (ILM), a surprising finding as the lattice might be quite perfect defectless [71]. DB could be mobile, subsonic or otherwise, pinned or even impossible depending on parameter values in the potentials. Inside the phonon band they are not permitted since any resonance of their harmonics with the extended phonons will radiate them away. They can only appear below or above the phonon band. Accordingly, they cannot decay by emitting linear radiation/phonons. This is at variance with lattice solitons, corresponding to atomic lattice longitudinal elongations, which are generally supersonically moving localized excitations like those exhibited by the Toda or Morse lattices as we show below. If to longitudinal elongations we add onsite vibrations and, accordingly we add an onsite potential at each lattice site then the picture becomes rich of possibilities. For instance localized modes could be pinned or mobile depending not only on parameter values in the

Complimentary Contributor Copy

absolute sense but also on the ratio of the stiffness and depth of the intersite and onsite potentials involved in the dynamics. DB/ILM is to be expected when strong onsite potentials compete with weak intersite interactions. In this context it shoud be mentioned the polaron-breather concept as another extension of the original polaron idea. Two particular cases exist: a standard static polaron and a localized periodic lattice oscillation associated with a localized quasi-periodic electronic oscillation [72].

Figure 6 illustrates the supersonic traveling soliton found when the onsite potentials are switched off, whereas figure 7 illustrates the extreme opposite case when the intersite potentials are practically switched off and a pinned DB/ILM appears. The space-time evolution of localized excitations between these two extreme cases has been provided in ref. [73].

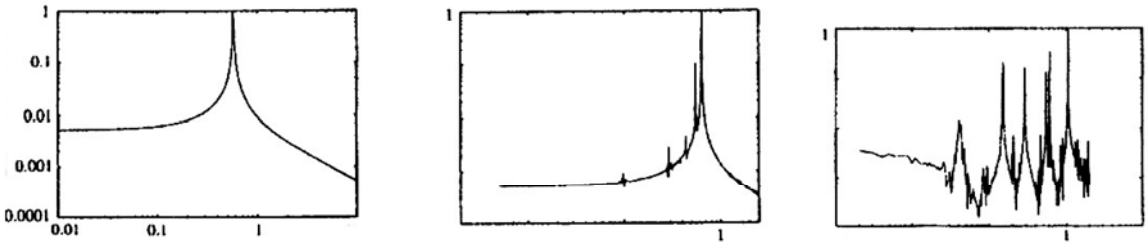


Figure 5. Morse lattice. Computed dynamic structure factor (suitably rescaled for illustrative purposes) against frequency (both in dimensionless units) with increasing temperature, respectively, below (left panel) at (center panel) and above (right panel) the expected transition, along the slopped region (0.1-1) in Figure 4, We can observe the transition from phonon to a messy background where the soliton emerges as the highest peak at extreme right. The value "1" along the abscissa indicates the dimensionless sound velocity and hence the soliton appears with supersonic speed.

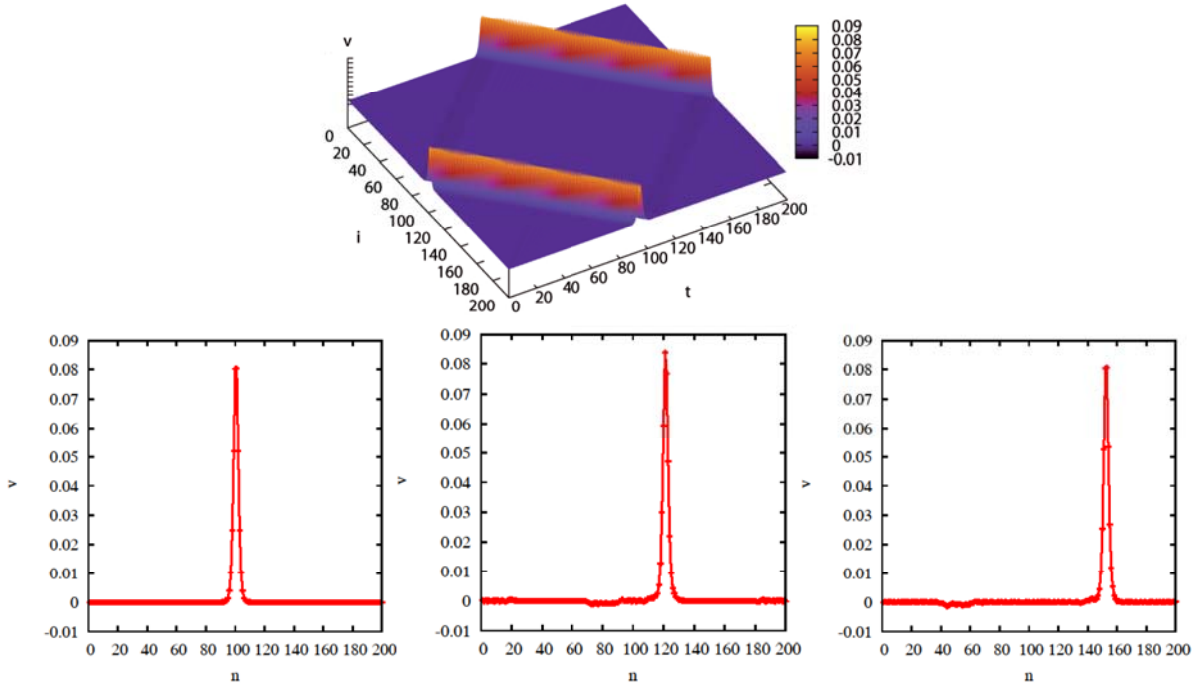


Figure 6. Morse lattice. Typical soliton in a 1d lattice with only intersite Morse interactions. The upper panel shows the actual motion along a lattice of two hundred units during two hundred time units (made dimensionless using as scale the inverse of the harmonic vibrations around the minimum of the Morse potential well). The lower panels illustrate, from left to right, the velocity v, as a defining quantity at time instants t = 10, 20 and 50, in appropriate dimensionless units. Motion is supersonic with value 1.05 the sound velocity. (Adapted from [73] with the permission of EDP Sciences).

Complimentary Contributor Copy

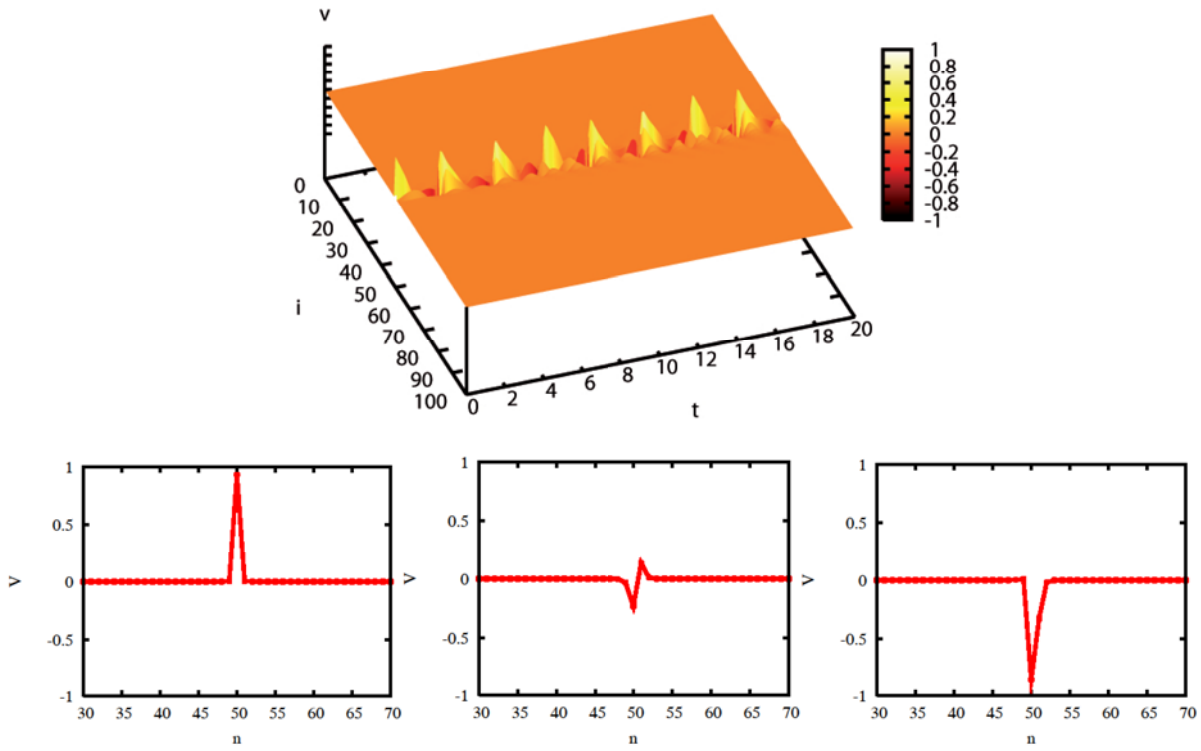


Figure 7. Morse lattice. Typical DB/ILM in a 1d lattice with strongly dominating onsite Morse interactions. The upper panel shows the actual motionless character of the local excitation. The lower panels show how there is local periodic alternance between a maximum and a minimum as time proceeds, for time instants t = 0.1, 1.2 and 2 in appropriate dimensionless units. (Adapted from [73] with the permission of EDP Sciences).

3.2. Electron Surfing on Nanoscale Lattice Solitons

Now we consider the role of the Morse interactions, and hence the role of lattice solitons, on the transport of electrons. Thus, we introduce an additional excess electron into the lattice crystal system. Figure 8 qualitatively shows the electric polarization field consequence of a local compression along the crystal lattice as horizontal axis, denoted *y*. In the reference frame of the atoms, this lattice deformation or distortion as it moves appears as a soliton correlated to a polarization wave (polarization and lattice distortion can be used to account for the same conceptual consequence). There is a "single" deepest well/trough whose depth depends on the actual local lattice compression (stronger in the left panel relative to the right panel). Otherwise all the troughs would have the same depth and would be placed one at each atom site. If atoms were considered moving (c_{ion} to the right) then the solitonic wave moves (c_{wave}) in the opposite direction to that of the overall atomic motions. Such a behavior is quite the same as that of the solitonic bore wave (hydraulic jump) in a river which travels upstream while the water flows downstream towards, say, the sea. Here the added, excess electron would fall in the deepest trough and, only in it, would be moving bound to it as a surfing motion.

Complimentary Contributor Copy

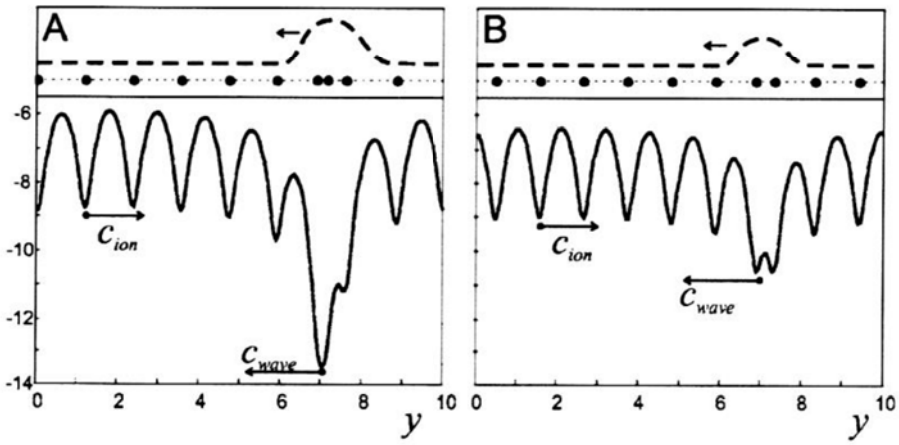


Figure 8. Morse lattice. The upper portion in the left panel corresponds to three atoms compressed to being quite near to each other whereas in the right panel the corresponding compression is weaker and affects only a couple of atoms. The middle horizontal rows show the atoms along the lattice assumed to move left to right with velocity c_{ion}. The lower portions of the panels depict the corresponding traveling polarization field in the form of solitonic wave, moving right to left, with velocity c_{wave}. These two velocities are here inserted to clearly illustrate the fact the solitonic wave travels opposite to the given motion of the atoms in the crystal lattice.

To substantiate the above sketched heuristic argument, on the one hand we replace in Eq. (1) the lattice intersite potential and on the other hand to recall the role of onsite energies/potentials here we replace the third term of (1) by the more complete electron contribution

$$H_e = \Sigma_n \varepsilon_n(q_n) c_n c^*_n - \Sigma_n t_{n+1,n}(q_n)(c^*_{n+1} c_n + c^*_n c_{n+1}) \tag{22}$$

with $\varepsilon_n = \varepsilon^o_n + \chi_o q_n + \chi_1 (q_{n+1} - q_{n-1}) + \ldots$ and here

$$t_{n,n-1} = t_o exp[-\alpha(q_n - q_{n-1})] \tag{23}$$

where, following Slater [23, 24], the matrix elements (overlapping or hopping integrals between nearest-neighbors) are taken in exponential form. Clearly, Taylor expanding (23) and (5) in the first approximation we get the corresponding component of the SSH Hamiltonian (1)-(2). The parameter α regulates how much the $t_{n,m}$ are influenced by the corresponding intersite separations, $(q_n - q_{n-1})$. In the simplest case it is enough to account for the compound product αt_0 as in (1). Note the different units of α in Eqs. (2) and (23).

To make the description of universal value we rescale all quantities using new units. Thus we set $t = t_o/2D$, $\tau = t_o/\hbar\omega_M \sim 10\text{-}20$ and $\varepsilon_o = \varepsilon^o_n/\hbar\omega_M$. Accordingly, in terms of energy we have:

$$\varepsilon_e = [\varepsilon^o_n + \chi_o q_n + \chi_1 (q_{n+1} - q_{n-1})] |c_n|^2 - 2\tau \Sigma_n Re(c_{n+1} c^*_n) exp\alpha(q_n - q_{n+1}) \tag{24}$$

Then from the Hamiltonian now incorporating Morse lattice intersite interactions and the electron-lattice interactions the following equations of motion are obtained:

Complimentary Contributor Copy

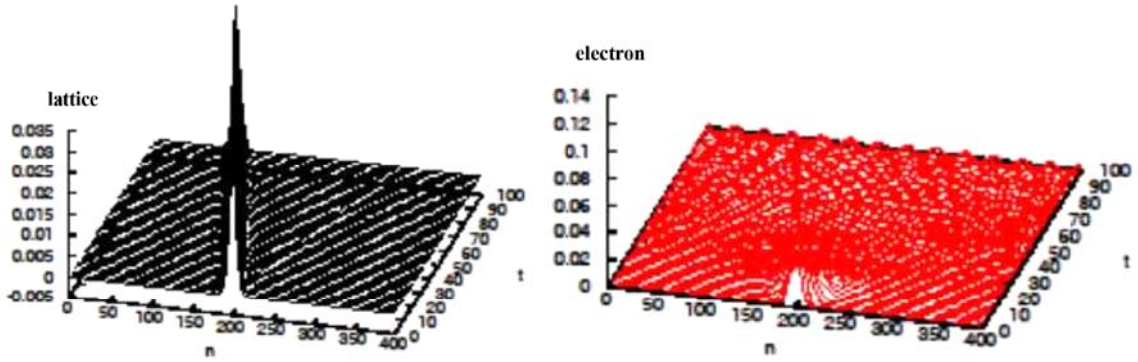


Figure 9. Morse lattice. Left panel: Lattice soliton evolution according to Eq. (25) with $\alpha = t_0 = 0$. Right panel: Evolution of an electron as provided by Eqs. (26) when also $\alpha = t_0 = 0$. Initially both are localized at site 200. As time proceeds, the soliton evolves almost unaltered whereas the electron peaked at the initial time "uniformly" spreads all over the lattice in accordance with the lattice discretized Schrödinger equations (26). (Adapted from [54] with the permission of AIP Publishing).

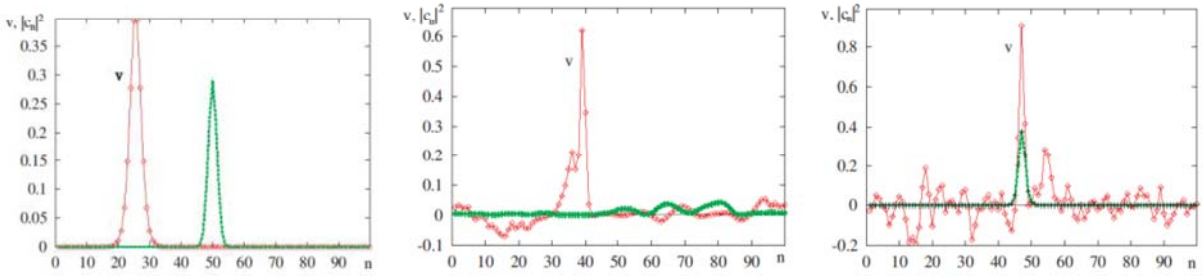


Figure 10. Morse lattice. Extreme left and center panels: Initial and final outcome of the evolution of the lattice soliton and the "excess albeit free" electron as depicted in the preceding Figure 9, when $\alpha = t_0 = 0$. Extreme right panel: Once the final states are those of the center panel, the electron-lattice interaction is switched on and hence when α and t_0 are nonvanishing, the soliton via Eqs. (25) and (26) dynamically gathers the tiny (practically) uniform electron probability density (satisfying the lattice discretized Schrödinger equations) piling it up to a peak around itself (kind of vacuum cleaner process) and then travels as a solectron bound state. (Adapted from [54] with the permission of AIP Publishing).

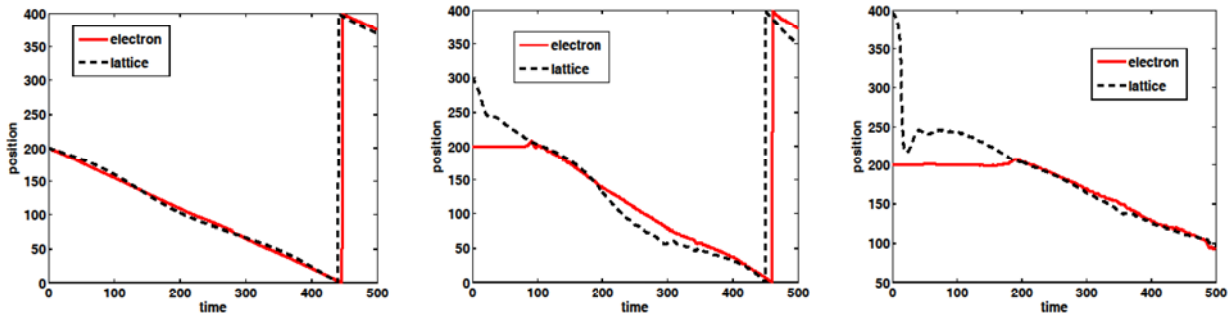


Figure 11. Morse lattice. Sketch of the space-time trajectories of the soliton and the electron. When α and t_0 are nonvanishing, when the former is placed at sites 200, 300 and 400 whereas the latter is always localized at site 200 at the initial time. Following a short transient the soliton manages to catch the electron (in probability density) thus forming the solectron bound state. Needless to say there is also a polaron process which we do not consider here for simplicity. (Adapted from [54] with the permission of AIP Publishing).

Complimentary Contributor Copy

$$d^2q_n/dt^2 = [1-\exp(q_n-q_{n+1})]\exp(q_n-q_{n+1})-[1-\exp(q_{n-1}-q_n)]\exp(q_{n-1}-q_n)+ 2\alpha t_0[Re(c_{n+1}{}^*c_n)\exp\alpha(q_n-q_{n+1})-Re(c_nc^*{}_{n-1})\exp\alpha(q_{n-1}-q_n)]+(t/\tau)[-\chi_o|c_n|^2+\chi_1(|c_{n+1}|^2-|c_{n-1}|^2)] \quad (25)$$

$$i(dc_n/dt) = [\varepsilon^o{}_n+\chi_o q_n+\chi_1(q_{n+1}-q_{n-1})]c_n-\tau[c_{n+1}\exp\alpha(q_n-q_{n+1})+c_{n1}\exp\alpha(q_{n-1}-q_n)]-(n-n_{el})Ec_n \quad (26)$$

The latter is the lattice discretized Schrödinger equation. For completeness we have added an external electric field, with E and $\hat{E}$ such that $E = (h\omega_M/\sigma e)\hat{E}$(V/m). It seems clear that external electric field is capable of altering the lattice dynamics and hence affecting acoustic excitations (waves, phonons, solitons) in the system.

The equations (25) and (26) are a mixed classical-quantum system that is to be integrated using appropriate periodic boundary conditions, $q_{N+1} = q_1$ and $dq_{N+1}/dt = dq_1/dt$, and initial conditions, recalling the conservative character of the dynamics and the probability density constraint for the electron $\Sigma_n |c_n|^2 = 1$. To a first approximation we can restrict to $\chi_o = \chi_1 = 0$ and $\varepsilon^o{}_n$ can be eliminated by rescaling the reference energy level. Then following a short transient quickly the electron of (26) (in probability density) is trapped by the soliton wave of (25) thus forming a bound state which is the solectron. As for the SWAP case discussed in the preceding section, this solectron is indeed a further generalization of the polaron concept (and charge carrier). Here, however, we have the electron surfing on the mechanical, acoustic lattice soliton wave that exists alien to the presence of the added excess electron. Clearly, this is at variance with both the polaron and the SWAP concepts where it is the electron that selftraps, thus creating the new charge carrier; both are electronically induced crystal lattice excitations. In the present case one expects indeed the action of the two influences, polaronic and solitonic but we shall not dwell on this matter here, referring the reader to [57].

Figure 9 illustrates how a soliton and an electron evolve separately in a Morse crystal lattice. Figures 10 and 11 offer alternative views. Noteworthy is that if the Schrödinger equation is integrated separately alone ($\alpha = t_0 = 0$), as time proceeds the electron "diffusively" becomes delocalized all over the lattice ring (Figure 10, center panel). Then when, after the delocalization is established, α and t_0 are made non zero hence switching on the electron lattice/soliton/phonon interaction, soon the electron becomes trapped by the lattice soliton as the latter forces reconstruction of a peaked electron probability density around itself in a kind of "vacuum cleaner" process (Figure 10 extreme right panel). We have a clear case of mechanical control of electros at the nanolevel [75].

3.3. Consequence of Electron Surfing

Figure 12 gives the results of a computer simulation to explain the earlier mentioned experimental findings of Donovan and Wilson [46-49]. It considers a 400 unit one-dimensional lattice and applies Eqs. (25) and (26). As an initial condition at $t = 0$ is taken the known analytical form of the soliton of the Toda lattice $exp[3(q_n-q_{n+1})] = 1+\beta^2/\cosh^2(\kappa n-\beta t)$, with the corresponding formula for its velocity; $\beta = \sinh\kappa/\kappa$ and κ is its mid-height inverse width (in units $1/\sigma$). Further, at $t = 0$ the electron probability density (normalized to unity, $\Sigma_n|c_n|^2=1$ is taken as a Gaussian distribution, centered at site n_{el}, with a width σ_{el}, which is

Complimentary Contributor Copy

approximately that of the chosen soliton initial condition; in practical terms $\sigma_{el} = 3$ and $\tau = 10$ in all the computations. For simplicity we set $\chi_o = \chi_1 = \varepsilon^o_n = 0$. Other values used are $M \sim 10^{-22}$g, $D \sim 0.03\text{-}0.3$eV, $b \sim 2\text{-}5 Å^{-1}$, $t_o < 1$eV, $\omega_M \sim 5.10^{12}\, s^{-1}$ and $\omega_e \sim 10^{14} s^{-1}$. Also for simplicity, the soliton and the electron are placed at lattice site 100 to rule out boundary effects. This is not a limitation since, as earlier illustrated, wherever the electron is placed along the lattice, the soliton placed in the same or different site is always able to trap it.

In accordance with the theory presented above, after a short transient, there is the formation of a bound state of the soliton with the electron which is the solectron. The solectron velocity (in units of sound velocity) is estimated as the slope of its trajectory in the space-time (n, t) plot. Figure 12 (left panel) depicts the solectron velocity v_s against the compound parameter αt_0 (in Eq. 25) accounting for the electron-lattice interaction. As expected, the latter affects the soliton with, however, supersonic values in a significant range ($0 < \alpha t_0 < 0.3$). In Figure 12 (right panel) there is a domain up to, say, $E = 0.1$ where the drift velocity is field independent for quite a wide range of values of the field strength. On the other hand, in the subsonic case the drift velocity grows with the increasing field value reaching saturation at the sound velocity. That panel also shows two significant consequences. First, as the field strength goes down, an ultrahigh mobility is expected, in agreement with the earlier mentioned experimental results found by Donovan and Wilson [46-49]. Second, the electric field appears as a (left-right) symmetry-breaking agent. Indeed, in general, as motion is always expected even in the absence of an external electric field, once the soliton is excited, as solitons, and hence the solectrons, can move to the left or to the right, on the average no net conduction would be the outcome. Switching on the field breaks the symmetry thus allowing one or the other to be realized.

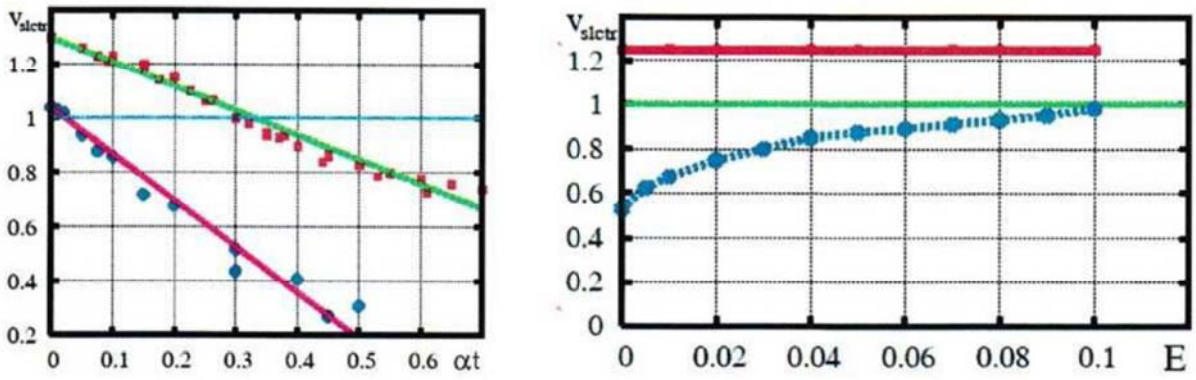


Figure 12. PDA. Left panel: solectron velocity, v_{slc} against the electron-lattice interaction parameter αt, for $\kappa = 0.5$ with initial $v_{soliton} = 1.04$ (pink/bottom line) and for $\kappa = 1.3.5$ with initial $v_{soliton} = 1.3$ (green/upper line). Dots are computer results and straight lines approximate fits for illustration, $v_{slc} = 1.3\text{-}0.9\alpha t$ (upper line) and $v_{slc} = 1.04\text{-}1.7\alpha t$ (lower lines). Right panel: dimensionless subsonic (blue/lower curve) and supersonic (red/upper line) solectron velocity against dimensionless field strength. The green/horizontal line at the value unity corresponds to the (linear) sound velocity. For illustration E = 0.1 corresponds to $E = 10^6$V/m. (Adapted from [74] with the permission of EDP Sciences).

Finally, note that the solectron transport theory outlined in subsections 3.2 and 3.3 offer universality. Indeed, besides the application to PDA, it can be used for other materials whose crystal vibrations permit strong enough compressions capable of exhibiting soliton

Complimentary Contributor Copy

excitations. Let us insist that it is a clear case of mechanical control of electrons at the nano-scale [75].

4. A Novel Field Effect Transistor as a Practical Application of electrOn Surfing

Worth noting is that if both the expression of the Morse potential (21) and that of the Slater's overlapping integral (23) are taken in appropriate approximations, then we go to the Davydov's approach or to the SSH description (save the degeneracy of the ground state) thus leading to Wilson's SWAP theory. One way or the other we have a soliton assisted (solectron) charge transport. Accordingly, it is of interest to consider the possibility of using the propagation properties of the solectron in novel new devices, which may complement devices using the propagation of electrons. We now describe the design of a new field effect transistor using the solectron properties [SFET-Solectron Field Effect Transistor and Inverter, GB2533105 A- 15.06.2016 UK patent pending; MG Velarde and EG Wilson, co-inventors], and compare its properties to the existing silicon field effect transistors (SiFET).

The proposed SFET uses an insulator, which if injected with an electron, forms a solectron, which propagates at around the sound velocity, in a preferred direction, set by the insulator properties. The source to drain channel lies along this preferred direction. The distance of ballistic flight of the solectron is greater than the channel length. Thus, there is severe constraint in material suitable for the SFET (as there is, of course, for the SiFET). As expected from the theory and arguments presented in the preceding sections possible candidates fulfilling these restrictions are the polydiacetylene (PDA) family of polymer perfect single crystals.

In Figure 13 metallic source and drain electrodes are evaporated onto the surface of the solectron supporting crystal, using appropriate masks to create the desired metal shapes. The masks are orientation relative to the crystal such that the solectron preferred propagation direction is oriented along the channel from source to drain. An insulator layer is then evaporated or spin coated. Finally the gate metal is evaporated. The source, drain and gate metals are identical and chosen to have a lower work function than the crystal electron affinity. Thus, the source and drain metals, in thermal equilibrium, inject electrons into the conduction band of the crystal, which then form solectrons.

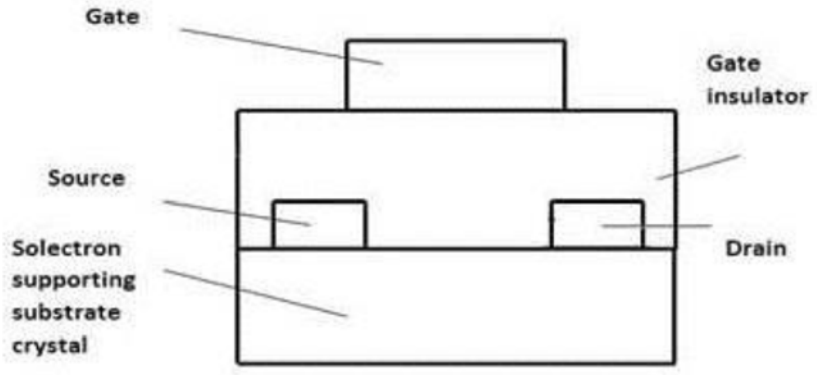


Figure 13. The source, drain, and gate are the conductors of the three terminal transistor.

Complimentary Contributor Copy

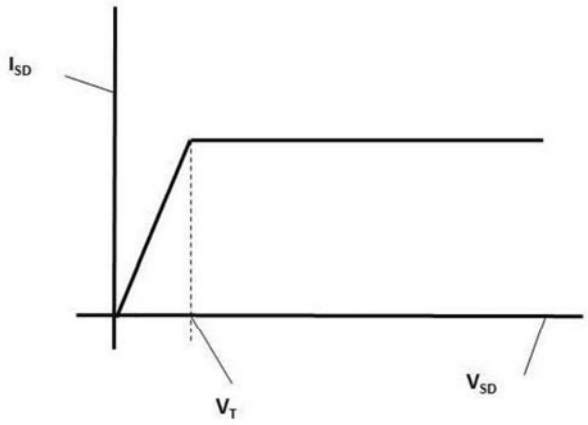


Figure 14. The source to drain current I_{SD}, against the source to drain voltage V_{SD}, at constant gate to source voltage.

Figure 14 shows a graph of the source–drain current I_{SD}, against the source – drain voltage V_{SD}. The voltage V_T is (kT/e) = 25 mV. For $V_{SD} > V_T$ the current is carried by solectrons moving from source to drain at constant velocity. The voltage along the channel does not change. The solectron density along the channel does not change. For $V_{SD} < V_T$ the current falls, as solectrons of thermal energy under the drain can enter the channel and reach the source. Continuing increase of $V_{SD} > V_T$ does not change the channel voltage; or current; rather, a voltage fall, in a small length adjacent to the drain is increased in value.

Figure 15 shows a graph of the source – drain current, I_{SD} against the source–gate voltage, V_{SG}. Solectrons under the source of thermal energies kT require the gate voltage to be $-V_T$ to stop them entering the channel. However, due to the distribution of energies of solectrons, about the average of kT, the current will not be abruptly zero as V_{SG} is reduced. It is important to stress that the source to drain, D, current, I_{SD}, is carried by injected charge from the source. This injected charge is not in thermal equilibrium with the insulator electron states or with insulator dopant electron states. This is in contrast to the SiFET where the channel charge is in local thermal equilibrium, such charge residing in dopant electron states or the conduction band.

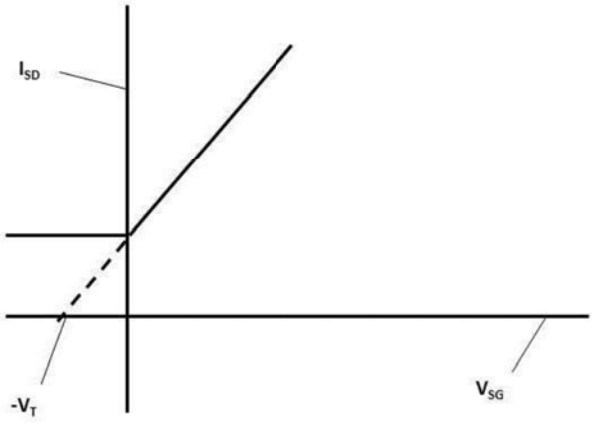


Figure 15. The source-drain current I_{SD} against the source-gate voltage V_{SD} at constant source drain voltage.

Complimentary Contributor Copy

The limit to the response time of the SFET is the transit time, T, from source to drain. For example, for a solectron velocity of $v = 2 \times 10^3$ m/s, and a source–drain distance of $L = 0.05$ μm, then

$$T = L/v = 0.025\ ns \tag{27}$$

The capacity between gate and channel, C, depends on the gate area, which for a SFET of width W cannot be smaller than WL. C also depends on the dielectric constant of the layer between gate and channel, ε, and the thickness, d, of the insulator layer according to

$$C = \varepsilon\varepsilon_0\, WL/d \tag{28}$$

The distance d is constrained only by being of order L or less. This is in contrast with the SiFET, which requires field from the gate to enter the semiconductor in order to change the local thermal equilibrium, and hence carrier densities. It the gate insulator is too thick, insufficient field enters the semiconductor to effect such change. Thus, the gate to channel insulator capacity, C, can be much smaller in the SFET than the SiFET.

The transfer conductance G, is defined here as the change of source - drain current in response to change of the gate – source voltage, e.g.,

$$G = (dI_{SD}/dV_{SG}) = C/T = \varepsilon\varepsilon_0\ v\ (W/d) \tag{29}$$

Thus, G is dependent on only W and d and independent of L.

Table 2. Comparison of a silicon FET (SiFET) with a solectron FET (SFET). (a) Typical parameters for state of the art Intel Pentium chip (b) Choose same width and length as SiFET (c) Choose insulator thickness to equal source-drain length (d) The saturated velocity in n silicon (e) The solectron velocity (f) Choose same clock frequency and period as SiFET (g) The minimum usable clock period is limited by factors external to the SiFET

	SiFET (a)	SFET
source-drain length L/μm	0.05	0.05 (b)
width w/μm	0.2	0.2 (b)
insulator thickness/nm	2	50 (c)
Insulator dielectric constant ε	3.9 (SiO_2)	2
gate-channel capacity C/F	1.73×10^{-16}	3.54×10^{-18}
supply voltage VDD/volts	1	0.1
charge in channel Q/C	1.73×10^{-16}	3.54×10^{-19}
carrier velocity/ms^{-1}	6×10^4(d)	2×10^3 (e)
transit time T/ns	0.00083	0.025
channel current I/μA	208	0.0142
switch energy CV^2/Joules	1.73×10^{-16}	3.54×10^{-20}
switch energy CV^2/eV	1080	0.22
Clock frequency/GHz	3	3 (f)
Clock period/ns	0.33(g)	0.33 (f)

Complimentary Contributor Copy

The advantages of the SFET are twofold.

First, the source drain voltage, V, can be small, of order *(kT/e),* and the SFET still functions. This is because of the ballistic flight of the solectron; a field is not required along the channel to keep it moving. This is in contrast to the SiFET.

Second, the gate insulator thickness can be large, and yet small gate voltages can be used. This allows of a smaller gate to channel capacity, C.

These two factors are critical in the device energy consumption. The energy cost of a switch from ON to OFF in a FET as a component in an inverter, or in a Boolean logic gate, is CV^2. Thus, there are enormous gains in energy cost of computing to be gained due to reducing these two factors.

Table 2 displays the effect of these two factors when a numerical comparison is made between the silicon and the solectron FET. To affect the comparison a typical Intel Pentium chip SiFET is chosen, and compared to the SFET of the same width and channel length. It is important to note the larger gate insulator thickness and the smaller source drain voltage for the SFET, and the consequent reduction in the energy of switching.

CONCLUSION

In the preceding sections, we have recalled theoretical results concerning the evolution of a one-dimensional crystal lattice with an added excess electron when there is significant lattice deformation affecting the electronic structure of the crystal, which in turn drastically affects the electron states as a consequence of the electron-lattice/soliton/phonon interaction. This occurs either when the added electron forces the lattice deformation as in the original idea of the polaron concept, defined by Landau and Pekar and subsequent developers of the theory, or when due to a preexisting lattice deformation the electron is trapped in the already deformed electric polarization field associated to such lattice distortion. The standard polaron case occurs for crystal lattices with harmonic intersite interaction potentials. The case of intersite anharmonic interactions, like the Morse potential, offers the novelty of permitting the preexistence of a significant lattice deformation in the form of, e.g., lattice solitons that may appear as supersonic excitations although no added excess electron has been introduced. When in this other case the electron is added, the electron-lattice interaction leads to the generalization of polaron concept in the form of solectron, the latter due to the solitonic character of the crystal excitation. In such a dynamic situation there appears the possibility of field-free electron transport in certain range of parameter values. As a practical consequence of such form of transport, electron surfing with the soliton, there has been the invention of a solectron field effect transistor (SFET).

The claims of the invention are few and straightforward, with universality and not just limited to the above presented particular illustration using PDA and derivatives: 1) A field effect transistor in which the current carrier in the source-drain channel is an electron solectron which is a coherent particle formed from an electron and accompanying crystal lattice distortion. 2) A field effect transistor in which the current carrier in the source-drain channel is a hole solectron which is a coherent particle formed from a hole and accompanying crystal lattice distortion. And 3) an inverter constructed from the field effect transistors just mentioned.

Complimentary Contributor Copy

The inverter is predicted to operate at very low supply voltages. So also can circuits that rely on the inverter such as the Boolean logic gates used in computers. The gate–channel insulator thickness can be large, in comparison to the silicon field effect transistor (SiFET). For in the latter the insulator thickness is constrained to be increasingly small as both the supply voltage and hence the threshold voltage, are reduced. A larger insulator thickness is desirable as it leads to a smaller gate input capacity, and so less energy consumption on switching. It can operate at quite small currents, leading to rather low quiescent energy consumption. As the inverter is constructed from two SFET the energy cost of an inverter switch scales proportionally to the square of the supply voltage, and inversely proportional to the gate insulator thickness. Thus, in view of the above much lower energy consumption is predicted using SFET compared to current silicon technology.

Computation currently consumes many orders of magnitude more of energy in digital switching events than is theoretically necessary according to statistical physics [76, 77]; but the technology to reduce the consumption does not exist. The SFET offers a radically new idea to produce computer elements that enable switching with three orders a magnitude reduction in energy consumption. Its production will lead the way to substantial energy reductions by IT industries in use of digital computers, server farms, and smart phones.

REFERENCES

[1] Landau, L. D., 1933. *Phys. Z. Sowjetunion* 3, 664.
[2] Pekar, S. I. 1946., *J. Phys. USSR*10, 341.
[3] Pekar, S. I. 1946., *Zh. Eksp. Teor. Fiz./Soviet Phys. JETP*16, 341; 1948. *Ibidem* 18, 105.
[4] Landau, L. D., Pekar, S. I., 1948. *Zh. Eksp. Teor. Fiz./Soviet Phys. JETP* 18, 419.
[5] Pekar, S. I., 1954. *Untersuchungen über die Elektronentheorie* [*Investigations on the theory of electrons*], Berlin, Akademie Verlag (and references therein) [German translation from Russian original edition dated 1951].
[6] Rashba, E. I., in [7] (and references therein).
[7] Alexandrov, A. S., ed.2007. *Polarons in Advanced Materials*, Dordrecht, Springer (and references therein).
[8] Fröhlich, H. Pelzer, H., Zienau, S., 1950. *Phil. Mag*. 41, 221.
[9] Fröhlich, H., 1954. *Adv. Phys.*3, 325 (and references therein).
[10] Holstein, T., 1959. *Ann. Phys.*8, 325, 343 [reprinted 2000. *Ibidem* 281, 706, 725].
[11] Feynmann, R. P. 1955. *Phys. Rev.* 97,660.
[12] Firsov, Yu. A., 1975. *Polarons*, Moscow, Nauka (in Russian).
[13] Kaganov, M. I., Lifshitz, I. M., 1979. *Quasiparticles. Ideas and principles of Solid State Quantum Physics*, Moscow, Mir.
[14] Devreese, J. T. L., ed. 1972. *Polarons in Ionic Crystal and Polar Semiconductors*, Amsterdam, North-Holland (and references therein).
[15] Alexandrov, A. S., Mott, N. F., 1996. *Polarons and Bipolarons*, Singapore, World Scientific.

Complimentary Contributor Copy

[16] Yu. L., ed. 1992. *Solitons and Polarons in Conducting Polymers*, Singapore, World Scientific.
[17] Emin, D., 2013. *Polarons,* Cambridge, Cambridge Univ. Press.
[18] Wannier, G. H., 1959. *Elements of Solid State Theory*, Cambridge, Cambridge Univ. Press.
[19] Peierls, R. E., 1965. *Quantum Theory of Solids,* Oxford, Clarendon Press.
[20] Harrison, W. A., 1970. *Solid State Theory*, New York, Mc-Graw-Hill.
[21] Ascroft, N. W., N. Mermin, N. D., 1976. *Solid State Physics*, New York, Thomson Learning.
[22] Kittel, C., 2005. *Introduction to Solid State Physics*, 8th Ed., New York, Wiley.
[23] Slater, J. C., 1974. *Quantum Theory of Molecules and Solids*, vol. 4, New York, McGraw-Hill.
[24] Launay, J. P., Verdaguer, M., 2014. *Electrons in Molecules. From Basic Principles to Molecular Electronics*, Oxford, Oxford Univ. Press.
[25] Su, W. P., Schrieffer, J. R., Heeger, A. J., 1979. *Phys. Rev. Lett.*42, 1698.
[26] Heeger, A. J., Kivelson, S., Schrieffer, J. R., Su, W. P., 1988. *Rev. Mod. Phys.*60, 781 (and references therein).
[27] Davydov, A. S., 1973. *J. Theoret. Biol*. 38, 559.
[28] Davydov, A. S., 1982. *Usp. Fiz. Nauk*138, 603 [1982. *Sov. Phys. Usp*. 25, 898] (and references therein).
[29] Davydov, A. S., 1991. *Solitons in Molecular Systems*, 2nd Ed., Dordrecht, Kluwer (and references therein).
[30] Zabusky, N. J., Kruskal, M. D., 1965. *Phys. Rev. Lett.*15, 57.
[31] Toda, M., 1967. *J. Phys. Soc. Japan* 22, 432; 23, 501.
[32] Toda, M., 1989. *Theory of Nonlinear Lattices*, 2nd Ed., Berlin, Springer.
[33] Chetverikov, A. P., Ebeling, W., Velarde, M. G., 2006. *Int. J. Bifurc. Chaos* 16,1613.
[34] Lomdahl, P. S., Kerr, W. C., 1985. *Phys. Rev. Lett.*55, 1238.
[35] Christiansen, P. L., Scott, A. C. eds., 1990. *Davydov's Soliton Revisited. Self-trapping of Vibrational Energy in Protein*, New York, Plenum.
[36] Scott, A. C., 1992. *Phys. Rep*. 217, 1.
[37] Cruzeiro-Hansson, L., Takeno, S., 1997. *Phys. Rev. E**56***, 894.
[38] Davydov, A. S., 1979. *Teor. Mat. Fiz.*40, 408 (in Russian).
[39] Davydov, A. S., Zolotaryuk, A. V., 1984. *Phys. Scr*. 30, 426.
[40] Zolotaryuk, A. V., Spatschek, K. H., Savin, A. V., 1995. *Europhys. Lett.*31, 531.
[41] Zolotaryuk, A. V., Spatschek, K. H., Savin, A. V., 1996. *Phys. Rev. B*54,266 (and references therein).
[42] Zmuidzinas, J. S., 1978. *Phys. Rev. B*17, 3919.
[43] Kosevich, Yu. A., 2017. *J. Phys. C: Conf. Series*833,012021.
[44] Kadantsev, V. N., Lupichev, L. N., 1990. *Phys. status solidi B* 161, 769.
[45] Lupichev, L. N., Savin, A. V., Kadantsev, V. N., 2015. *Synergetics of Molecular Systems,* Heidelberg, Springer.
[46] Donovan, K. J., Wilson, E. G., 1981. *Phil. Mag. B*44, 9; 31..

Complimentary Contributor Copy

[47] Donovan, K. J., Freeman, P. D., Wilson, E. G., 1985. *J. Phys. C: Solid State Phys.* 18, L275.
[48] Donovan, K. J., Wilson, E. G., 1990, *J. Phys.: Condens. Matter* 2, 1659.
[49] Donovan, K. J., Elkins, J. W. P., Wilson, E. G., 1991. *J. Phys.: Condens. Matter* 3, 2075.
[50] Wilson, E. G., 1983. *J. Physics C: Solid State Phys.*16, 6739.
[51] Velarde, M. G., Ebeling, W., Chetverikov, A. P., 2005. *Int. J. Bifurc. Chaos*15, 245.
[52] Velarde, M. G., Ebeling, W., Hennig, D., Neissner, C., 2006. *Int. J. Bifurc. Chaos*, 16, 1035.
[53] Hennig, D., Neissner, C., Velarde, M. G., Ebeling, W., 2006. *Phys. Rev. B*73, 024306.
[54] Hennig, D., Chetverikov, A. P., Velarde, M. G., Ebeling, W., 2007. *Phys. Rev. E 76*, 046602.
[55] Velarde, M. G., 2010. *J. Comp. Appl. Maths.* 233, 1432.
[56] Chetverikov, A. P., Ebeling, W., Velarde, M. G., 2016. *Eur. Phys. J. B*89, 196.
[57] Cantu-Ross, O. G., Cruzeiro, L., Velarde, M. G., W. Ebeling, W., 2011. *Eur. Phys. J. B*80, 545.
[58] Velarde, M. G., Ebeling, W., Chetverikov, A. P., 2008. *Int. J. Bifurc. Cha*os 18, 3815.
[59] Chetverikov, A. P., Ebeling, W., Velarde, M. G., 2009. *Eur. Phys. J. B*70, 217.
[60] Chetverikov, A. P., Ebeling, W., Velarde, M. G., 2010. *Int. J. Quantum Chem.* 110, 46.
[61] Brizhik, L. S., Davydov, A. S., 1984. *J. Low Temp. Phys.*10, 748.
[62] Brizhik, L. S., 1986. *J. Low Temp. Phys.*12,437.
[63] Brizhik, L. S., Eremko, A. A., 1995. *Physica D* 81, 295.
[64] Velarde, M. G., Brizhik, L. S., Chetverikov, A. P., Cruzeiro,L., Ebeling, W., Röpke, G., 2011. *Int. J. Quantum Chem.*112, 551, 2591.
[65] Brizhik, L. S. Chetverikov, A. P. Ebeling, W., Röpke, G. Velarde, M. G., 2012. *Phys. Rev. B* 85, 245105.
[66] Kobelt, D., Paulus, E. F., 1974. *Acta Crystallogr. B*30(1974) 232.
[67] Batchelder, D. N., Bloor, D., 1979. *J. Polymer Sci.*17, 568.
[68] Lochner, K., Bassler, A., Sowa, H., Ahsbahs, H., 1980. *Chem. Phys.*52, 179.
[69] Wilson, E. G., 1975. *J. Phys. C: Solid State Phys*. 8, 727.
[70] Batchelder, D. N., Bloor, D., 1978. *J. Phys. C: Solid State Phys.*11, L629.
[71] Dmitriev, S. V., Korznikova, E. A., Baimova, Yu. A., Velarde, M. G., 2016. *Phys. Uspekhi* 59, 446.
[72] Aubry, S., 1997. *Physica D* 103, 201
[73] Velarde, M. G. Chetverikov, A. P., Ebeling, W., Dmitriev, S. V., Lakhno, V. D. 2016. *Eur. Phys. J. B* 89, 233.
[74] Velarde M. G., Chetverikov, A. P., Ebeling, W., Wilson, E. G., Donovan, K. J., 2014. *Europhys. Lett.-EPL* 106, 27004.
[75] Velarde, M. G., 2016. *Eur. Phys. J. ST*225, 921.

Complimentary Contributor Copy

[76] Landauer R., 1961. *IBM J. Res. Dev.* **5**, 183 [Reprinted 2000. *Ibidem* 44, 261].
[77] Vacarro, J., Barnett, S., 2011. *Proc. Roy. Soc. A* 467, 1770.

Complimentary Contributor Copy